Vibrational Spectroscopy 103 (2019) 102932

Contents lists available at ScienceDirect

Vibrational Spectroscopy

journal homepage: www.elsevier.com/locate/vibspec

Mucin structural interactions with an alginate oligomer mucolytic in cystic fibrosis sputum

Manon F. Pritchard[a], Juliette L. Oakley[a,*], Charles D. Brilliant[b], Philip D. Rye[c], Julian Forton[d], Iolo J.M. Doull[d], Ian Ketchell[e], Katja E. Hill[a], David W. Thomas[a], Paul D. Lewis[b]

[a] Advanced Therapies Group, Cardiff University School of Dentistry, Heath, Cardiff, UK
[b] Respiratory Diagnostics Group, Medical School, Swansea University, Swansea, UK
[c] AlgiPharma AS, Sandvika, Norway
[d] Respiratory/Cystic Fibrosis Unit, Children's Hospital for Wales, Cardiff, UK
[e] Adult Cystic Fibrosis Unit, Llandough Hospital, Cardiff, UK

ARTICLE INFO

Keywords:
Alginate oligomer
Cystic fibrosis
FTIR
Mucin
Sputum

ABSTRACT

Cystic fibrosis (CF) is an autosomal recessive, life-limiting condition characterized by progressive lung disease, which is a major cause of morbidity and mortality for these patients. The inhalation therapy, OligoG CF-5/20, is a low molecular weight (mean Mn 3200 g/mol) alginate oligomer, with a high guluronic acid content (> 85%). The ability of OligoG CF-5/20 to enhance the activity of antimicrobial/antibiotic therapies, modify the rheological properties of CF sputum and interact with mucin, has previously been shown. To further characterize the physicochemical interactions of OligoG CF-5/20 with CF sputum, Fourier-transform infrared (FTIR) spectroscopy was used to analyze *ex vivo* sputum samples from adolescent CF patients (n = 13) following treatment with 0.2% OligoG CF-5/20. FTIR analysis confirmed the interaction of OligoG CF-5/20 with mucin glycans in CF sputum, which showed a shift in wavenumber from 1078 cm^{-1} to 1070 cm^{-1} and subsequent loss of the 1053 cm^{-1} peak in the OligoG CF-5/20 treated samples. OligoG CF-5/20 interaction with key terminal moieties in mucin were also evident, with a significant change in sulphation at wavenumber 1116 cm^{-1}, suggesting a link with sulphated Lewis x antigen. There were also significant shifts at wavenumber 1637 cm^{-1} indicative of β-sheet conformational changes in the mucin peptide caused by action of OligoG. The alterations in charge of glycan and mucin structures support previous observations wherein OligoG CF-5/20 modifies the viscoelastic properties of CF sputum. These findings suggest a possible mechanism of action for the rheological changes observed with this novel therapy.

1. Introduction

Cystic fibrosis (CF) is an autosomal recessive disorder affecting 1 in 2500 live births in the UK [1]. This life-limiting condition (median predicted survival age ~47 years) [2] is the result of mutations in the CF transmembrane conductance regulator (CFTR) gene, characterized by impaired epithelial chloride transport, leading to an abnormally viscous mucous and poor lung clearance [3]. Obstructive pulmonary disease is the primary cause of morbidity and mortality (~80%) within CF patients [4]. The ongoing cycle of infections caused by this thick, often stagnant, mucus in the lung necessitates chronic use of antibiotics. Patients eventually become colonized by multi-drug resistant (MDR) pathogens, particularly *Pseudomonas aeruginosa*, leading to chronic inflammation and reduced lung function [5]. Within the diseased CF lung, the viscoelasticity of mucus is altered by constituents such as lipids, proteins (e.g. IgM), DNA and mucins [6].

Mucins are a large glycosylated protein component of mucus [7]. Although mucins represent < 1% (w/v) of respiratory secretions [8–10], they are important gel-forming constituents in CF sputum [11–13]. They also play an important role in the innate immune system [14] both as a physical barrier against chemical, enzymatic and mechanical insult, and by providing a 'first line' of defense against pathogens [15]. Whilst important in defense, mucin barriers may impede drug delivery; with inhaled agents binding to the mucins and being rapidly removed by mucociliary clearance [16]. Methods to disrupt these muco-adhesive interactions, allowing crossing of the mucin-protective layer of the lung, would greatly improve drug delivery [17].

Alterations in terminal carbohydrate moieties are associated with

* Corresponding author.
E-mail address: oakleyjl2@cardiff.ac.uk (J.L. Oakley).

https://doi.org/10.1016/j.vibspec.2019.102932
Received 10 March 2019; Received in revised form 31 May 2019; Accepted 11 June 2019
Available online 12 June 2019

respiratory disease and these modifications cause changes in the viscoelastic properties of the mucus, as the addition of charged residues influences mucin aggregation [18]. CF mucins have been shown to possess increased levels of fucose, galactose, *N*-acetylglucosamine [19], sialic acid and sulphate [12]. Furthermore, increases in glycosylation and branching in CF mucins have been shown to result in a higher tendency to 'gel' and obstruct transport *in vivo* [19]. It has also been demonstrated in CF that mucins may exhibit increased levels of expression of sialylated and sulphated-Lewis x determinants during inflammation and infection [8]. The sulphated Lewis x antigen is the main sulphated sugar in CF respiratory mucin [18]. Over sulphation in CF respiratory and salivary mucins has long been reported in the literature [20–23].

OligoG CF-5/20 is a low molecular weight oligosaccharide derived from the stem of brown seaweed, *Laminaria hyperborea*, and has recently completed Phase 2b clinical trials (NCT02157922; NCT02453789) as an inhalation therapy for CF patients. In previous *in vitro* studies, treatment with G-rich alginate oligomers was shown to alter the viscoelastic properties of mucin/alginate gels, mucin/DNA gels and CF sputum [24,25]. OligoG CF-5/20 interacts with respiratory mucins, inducing alterations in mucin porosity and surface charge [25]. It has also been shown to potentiate antibiotics against a range of multidrug resistant bacteria (up to 512-fold) [26]. Further studies have confirmed its ability to alter the surface charge of *P. aeruginosa* leading to bacterial aggregation, a reduction in bacterial motility, and impaired biofilm formation [27,28]. High MW alginate as secreted by virulent CF respiratory bacteria such as a mucoid *P. aeruginosa*, increase the elasticity and viscosity of mucus, whilst conversely, low Mw alginates have been shown to reduce the bulk elasticity and viscosity of mucus [29]. Interestingly, *in vitro* and *in vivo* studies have shown that low Mw alginate oligosaccharides are able to displace mucin-high MW alginate interactions, as might be expected to occur in the chronically infected lung.

This study used Fourier-transform infrared spectroscopy (FTIR) to examine direct physicochemical interactions of OligoG CF-5/20 with respiratory mucins in order to better understand how it is able to alter CF sputum viscosity. FTIR is a low-cost, high-throughput optical technology which requires only low volumes of test samples and has previously been employed to accurately characterize alterations in mucin expression, secretion and glycosylation (as well as in the Lewis x antigen structures) in respiratory disease [18,30,31].

The aim of this study was to use mucin infrared (IR) profiles from our extensive spectral library (18), to identify key IR markers to describe the structural changes and electrostatic interactions that occur within mucin glycan moieties and peptide backbone following OligoG CF-5/20 treatment of CF sputum.

2. Materials and methods

2.1. Patient samples

Induced sputum samples were collected from cystic fibrosis patients after obtaining informed written consent (CF Sputum Induction Trial [CF-SpIT] UKCRN: 14615). FTIR samples were collected from 13 patients (mean age 13.1 years; range 7–17 years; male to female ratio, 9:4 respectively). The mean FEV_1 (% predicted) was 73 (range 31 to 99%) with 69% of patients found to be infected with *P. aeruginosa* at the time of sampling (Table 1). Samples were collected by expectoration, after which they were stored by freezing at −80 °C. Prior to subsequent use, sputum samples were defrosted overnight at 4 °C.

2.2. Fourier-transform infrared spectroscopy of cystic fibrosis sputum

FTIR analysis was performed on CF patient sputum samples (n = 13 patients; Table 1) + 0.2% OligoG CF-5/20 or dH_2O; 0.2% OligoG CF-5/20 reference spectra were also generated. CF sputum was incubated with 0.2% (w/v) OligoG CF-5/20 or dH_2O (control) for 4 h at 37 °C [25]. 3 µl of each sample was pipetted in triplicate onto a 96-well silicon plate (Bruker Optics Inc., Coventry, UK). Following drying at room temperature (1 h), high-throughput FTIR analysis was performed using a Bruker Vertex 70 in transmission mode with a KBr beamsplitter, DTGS detector and HTS-XT attachment. Spectra were acquired within the range of 4000-400cm^{-1}, at a resolution of 4 cm^{-1} with each spectrum being the averaged result of 32 scans. Each silicon plate was scanned in triplicate to ensure reproducibility of individual sample spectra.

All data processing, analysis and visualizations were performed using Bruker OPUS 7.5 software, and the R-statistical computing environment using in-built algorithms and code developed by our group. The whole infrared spectra were pre-processed prior to further analysis by baseline correction using the automatic 'rubberband' correction and vector normalization. Absorbance spectra were smoothed using a nine-point Savitzky-Golay algorithm and second derivative spectra were calculated using a 9-point window. Based on our previously developed mucin glycosylation IR spectral library (18), we assessed the 'fingerprint' spectral region (absorbance values between wavenumbers 1800 and 900 cm^{-1}). Statistically significant differences between peak positions or absorbance intensity at key wavenumbers in treated and control CF sputum samples were determined using the Mann-Whitney *U* Test. Multiple hypothesis testing was carried out on all statistical test results using the Bonferroni correction. Whilst many potential wavenumbers were investigated during this study, only those wavenumbers which showed promise for determining interaction between OligoG CF-5/20 were statistically examined. The following wavenumbers were identified and statistically examined due to presence of peaks in treated CF sputum spectra but not OligoG CF-5/20 spectra: 1652, 1637, 1240, 1116, 1080 and 1053 cm^{-1}. Therefore, the corrected α-level was 0.008.

3. Results and discussion

FTIR was used to generate absorbance spectra between wavenumbers 400 to 4000 cm^{-1} to establish biochemical changes following 0.2% (w/v) OligoG CF-5/20 incubation with CF sputum samples. Analysis was then performed on IR wavenumbers within the 900 to 1800 cm^{-1} 'fingerprint' region to focus on key structural changes in mucin proteins and associated glycosylation. Fig. 1a shows the mean absorbance spectra for both untreated and treated CF sputum samples highlighting the wavenumber regions where IR absorbance patterns are altered post-treatment. The spectra were aligned with a representative OligoG CF-5/20 IR spectrum to easily identify regions of absorbance change that occurred due to OligoG CF-5/20 being present in the samples.

Raw absorbance IR spectra are a series of many peaks merged into broad peaks to determine the exact position of peak changes between untreated and OligoG CF-5/20 treated sputum spectra, whilst second derivative spectra are used to enhance the separation of any overlapping peaks. Second derivative spectra were calculated and aligned with that of OligoG CF-5/20 (Fig. 1b). Comparison of OligoG CF-5/20-treated and -untreated CF sputum second derivative spectra with a second derivative spectrum of 0.2% (w/v) OligoG CF-5/20 allowed determination of potential structural changes or interactions at key mucin peaks following OligoG CF-5/20 incubation of CF-patient sputum.

3.1. Mucin glycan changes in the presence of OligoG CF-5/20

IR peaks associated with mucin glycan moieties, including sialylated and sulphated Lewis x antigen, were initially assessed using known wavenumber absorbance data from our glycosylation IR spectral library [18]. Glycan associated structures, such as the C−O bonds in the pentose and hexose rings, absorb strongly between 900 and 1280 cm^{-1}, with numerous second derivative peaks being evident. Unfortunately,

Table 1
Patient data for sputum samples used for FTIR in this study.

Patient	Age (Years)	Sex	Antibiotics	Cultured Pathological Bacteria (Isolated in past 12 months)	FEV1 % predicted (Z score)	BMI centile (Z score)
1	16	M	AZM, FLC	*H. influenzae, S. aureus, S. maltophilia,*	62 (-3.2)	25 (-1.2)
2	17	M	AZM, CST^{IV}, FLC, DOX, MEM^{IV}, TOB^{neb}	*H. influenza, S. aureus, S. maltophilia,*	*	9 (-1.93)
3	14	F	AZM, CLR, ETB, RIF	*S. maltophilia*	64 (-3.0)	9 (-1.7)
4	15	F	AZM, CLM^{neb} FLC	*P. aeruginosa*	87 (-1.1)	50 (0.42)
5	15	M	AZM, CLM^{neb} FLC	*P. aeruginosa, S. aureus*	75 (-2.0)	25 (-0.99)
6	9	M	AZM, FLC, CLM^{neb}/TOB^{neb}	*S. marcescens, S. aureus*	84 (-1.3)	91 (1.23)
7	16	F	AZM, CLM^{neb}	*H. parainfluenzae*	64 (-2.9)	25 (-0.53)
8	14	M	CLR, MIN, MEM^{neb}, MXF	*M. abscessus*	57 (-3.5)	50 (0.2)
9	14	M	AZM	*H. influenzae, MRSA, S. aureus*	64 (-2.9)	91 (1.23)
10	11	M	AZM, CLM^{neb}	*P. aeruginosa, MRSA*	47 (-4.5)	50 (-0.49)
11	11	F		*B. cenocepacia*	99 (-0.1)	98 (1.96)
12	12	M	AZM	*P. aeruginosa (mucoid)*	78 (-1.8)	50 (0.34)
13	7	M	AZM, FLC, CLM^{neb}/TOB^{neb}	*B. cenocepacia, P. aeruginosa, S. maltophilia, S. aureus*	81 (-1.5)	91 (1.85)

Abbreviations: BMI centile, body mass index (kg/m2) centile; FEV1, forced expiratory volume in one second; IV, intravenous antibiotic; Neb, nebulised antibiotic. *Antibiotics: AZM*, azithromycin; *CLR*, clarithromycin; *CST*, colistin; *CLM*, colomycin; *DOX*, doxycycline; *ETB*, ethambutol; *FLC*, flucloxacillin; *MEM*, meropenem; *MIN*, minocycline; *MXF*, moxifloxacin; *RIF*, rifampicin; *TOB*, tobramycin.
Bacteria: *B. cenocepacia, Burkholderia cenocepacia; H. influenzae, Haemophilus influenzae; H. parainfluenzae, Haemophilus parainfluenzae; M. abscessus, Mycobacterium abscessus; M. avium-intracellulare, Mycobacterium avium-intracellulare, P. aeruginosa, Pseudomonas aeruginosa; S. aureus, Staphylococcus aureus; S. maltophilia, Stenotrophomonas maltophilia; S. marcescens, Serratia marcescens; MRSA, methicillin resistant S. aureus.*
* Missing data.

OligoG CF-5/20 also absorbs strongly within the same region as mucin glycans, with a number of key peaks identified at the same positions. As we were interested in determining sputum mucin-OligoG CF-5/20 interaction, and not just OligoG CF-5/20 presence in CF sputum, it was necessary to focus our analysis on wavenumbers that showed differences in absorbance, or peak presence which were not associated with OligoG peaks, as being indicators of OligoG CF-5/20 interaction. For example, Fig. 2a shows a second derivative peak at 1078 cm^{-1}, in the untreated sputum spectrum representing the major glycan-associated peak, shifted to 1070 cm^{-1} in the OligoG CF-5/20 treated sputum spectrum without a second derivative peak being evident in the OligoG CF-5/20 spectrum at the same wavenumbers. Fig. 2b shows that the distributions of major glycan-associated second derivative peak apex positions for all samples in the OligoG CF-5/20 treated sputum spectrum were significantly different from the untreated control samples (Table 2, $P < 0.008$). We also observed that a peak at 1053 cm^{-1} was completely lost following sputum treatment with OligoG CF-5/20, although comparison with the OligoG CF-5/20 spectrum shows presence of a peak maxima in the OligoG CF-5/20 spectrum. This suggests that the second derivative peak loss at 1053 cm^{-1} may not be indicative of interaction between OligoG CF-5/20 and the sputum mucins, rather it could be indicative of OligoG CF-5/20 presence.

We next assessed the wavenumber region surrounding 1116 cm^{-1} which we had previously identified as probable absorbance from the sulphated-Lewis x antigen [18]. Fig. 3a shows that absorbance at 1116 cm^{-1} was lost following OligoG CF-5/20 treatment, suggesting an interaction of OligoG CF-5/20 with the sulphated-Lewis x antigen. Fig. 3b, summarized in Table 2 shows significant differences across all samples between treated and untreated for 1116 cm^{-1}. We also examined absorbance at, and peak positions around, 1240 cm^{-1} which is

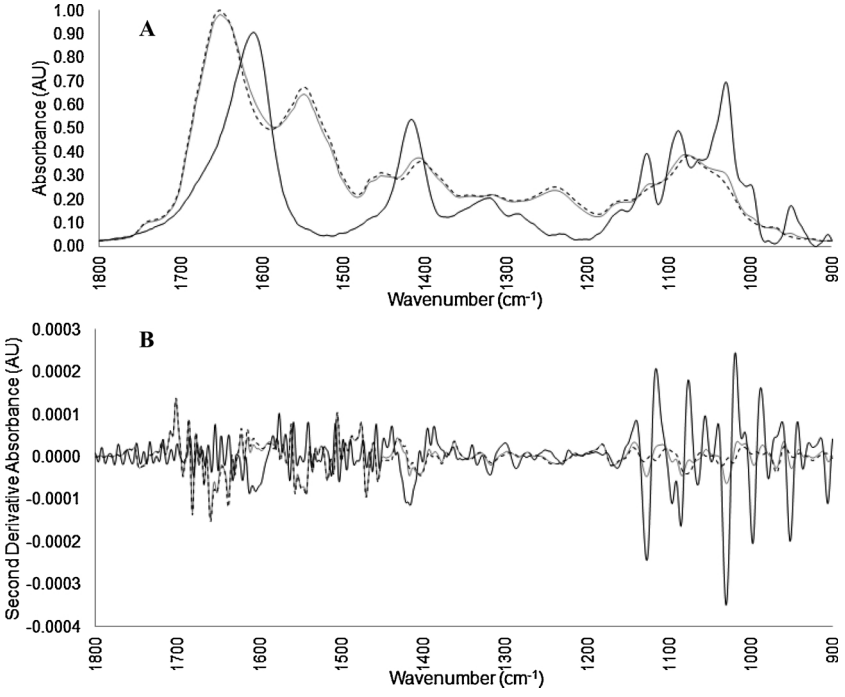

Fig. 1. Raw absorbance and second derivative infrared spectra for untreated and OligoG CF-5/20- treated sputum. (a) Mean IR spectra from the 1800 cm^{-1} to 1000 cm^{-1} IR wavenumber region of: untreated CF sputa; treated CF sputa; OligoG CF-5/20 in water. (b) Second derivative spectra for the above (note that peaks are negative and point down in second derivative IR spectra). Treated sputum, solid grey line; untreated sputum, black dashed line; OligoG CF-5/20, light-grey dashed line.

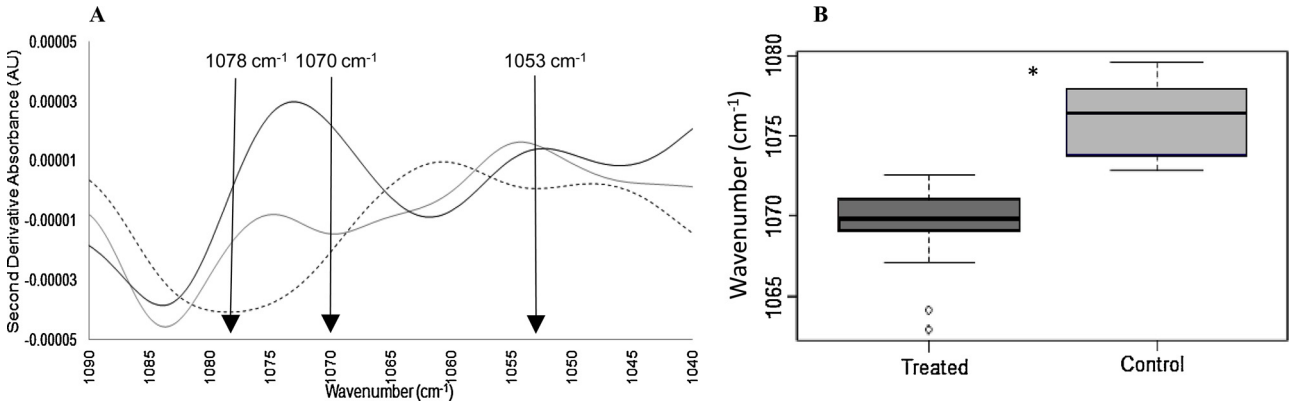

Fig. 2. Mean second derivative spectra for OligoG CF-5/20 treated and untreated sputum within the 1040 cm^{-1} to 1090 cm^{-1} wavenumber range indicating IR absorbance from mucin glycans and OligoG CF-5/20. (a) The IR peak at 1078 cm^{-1} shifted to 1070 cm^{-1} following OligoG CF-5/20 incubation and the peak at 1053 cm^{-1} in the untreated spectrum was completely lost. (b) Boxplots of peak positions between 1080 cm^{-1} and 1060 cm^{-1} show the distributions of second derivative peak apex positions centered around 1078 cm^{-1} and 1070 cm^{-1} in untreated and treated samples respectively. Treated sputum, solid grey line; untreated sputum, black dashed line; OligoG CF-5/20, light-grey dashed line. *P < 0.008, mean of n = 3 replicates.

Table 2
Results of Paired Mann-Whitney signed rank tests for differences of means in absorbance intensity at the specified wavenumbers, and peak position around the selected wavenumbers.λ = < 0.008 mean of n = 3 replicates.

Wavenumbers (cm^{-1})	Peak Shift or Absorbance Change	Mean Difference (Control – Treated)	p-value
1652	Second Derivative Peak Shift	0.3563 (cm^{-1})	0.5416
	Second Derivative Absorbance Change	3.246958* 10^{-6} (AU)	0.4731
1637	Second Derivative Peak Shift	0.3518 (cm^{-1})	0.0580
	Second Derivative Absorbance Change	$-2.016733 * 10^{-5}$ (AU)	0.0342
1240	Absorbance Peak Shift	0.0788 (cm^{-1})	0.3910
	Absorbance Change in Treated Group	0.00094 (AU)	0.0078 λ
1116	Second Derivative Peak Loss in Treated CF Sputum	NA	$3.436 * 10^{-11}$ λ
	Second Derivative Absorbance Change	$-2.795417 * 10^{-5}$ (AU)	$7.105 * 10^{-15}$ λ
1078	Second Derivative Peak Shift	−2.9444 (cm^{-1})	0.00012 λ
	Second Derivative Absorbance Change	$-2.186917 * 10^{-5}$ (AU)	$2.08 * 10^{-8}$ λ
1053	Second Derivative Peak Loss in Treated CF Sputum	NA	0.00001
	Second Derivative Absorbance Change	$-1.323538 * 10^{-5}$ (AU)	$1.052 * 10^{-10}$ λ

also indicative of absorbance by the sulphated-Lewis x antigen (Fig. 4a). A general but small shift in peak position towards lower wavenumbers in the OligoG CF-5/20 incubated sputum spectra, relative to untreated control sputum spectra (Fig. 4b) was observed. Additionally a small decrease in absorbance was observed at 1240 cm^{-1} in the incubated sputum spectra (Fig. 4c). Although this could suggest a likely interaction between OligoG CF-5/20 and sulphated-Lewis x antigen, the decrease in absorbance at 1240 cm^{-1} in the incubated sputum spectra, and the peak shift were not found to have statistical significance.

Within sputum, negatively-charged biopolymers such as mucin, DNA and alginates, assemble via physical entanglement of non-covalent bonds. As glycoproteins exhibit electrostatic, hydrophobic and hydrogen bonding interactions, mucin is able to readily adhere to other substances. Modification of the glycan chains of CF mucins has previously been hypothesized to increase bacterial binding and colonization in the CF lung. Alteration in mucin glycosylation has been demonstrated to potentiate *P. aeruginosa* binding to CF mucins when compared to non-CF mucins [32]. Glycan sulphation may increase with bacterial infection, possibly to protect the underlying glycoproteins from enzymatic degradation by bacteria [33]. Both inflammatory leukocytes and *P. aeruginosa* are thought to recognize sulphated ligands and lead to an inflammatory response and increased pathogenesis of *P. aeruginosa* respectively [21,34]. Interestingly, increases in sulphation have been demonstrated in the absence of bacterial infection in CF, suggesting this may be a primary defect of the disease [35,36]. However, other studies have reported a reduction in sulphation in CF patients when compared to healthy controls, leading some to dispute its significance in CF patients [37]. Nevertheless, changes in the sulphation peak in sputum observed in the current study suggest that OligoG CF-5/20 was able to bind to the sulphate moieties on the glycans, and in this way counteract the effects of pathogen recognition and binding [36].

Reducing barriers to drug and gene delivery [38,39] and modifying the properties of mucus may be beneficial in a range of clinical conditions such as CF [40], and reproductive medicine [41]. Although mucin generally serves as a barrier to bacteria, several pathogens such as *P. aeruginosa* reside within mucus and possess mucin-specific adhesins [17]. Mucin interactions with *P. aeruginosa* have been shown to increase bacterial motility, which is partly directed by both quorum sensing (QS) and the physical properties of mucin [42]. In contrast, OligoG CF-5/20 has been shown to bind to the cell surface of *P. aeruginosa,* modifying its QS signaling pathways and reducing its motility [26,28,43].

3.2. Mucin protein back bone changes in the presence of OligoG CF-5/20

To determine possible mucin peptide backbone alterations following incubation with OligoG CF-5/20, we examined the Amide I region between wavenumbers 1628 cm^{-1} and 1664 cm^{-1} (Fig. 5a). This range was selected to include those peaks related to the random coil (1652 cm^{-1}) and β-sheet (1637 cm^{-1}) secondary structures that predominate in sputum mucins and to avoid amino sugar absorbance at 1626 cm^{-1} [30]. Through FTIR analysis of these wavenumbers, we have previously shown OligoG CF-5/20 is capable of binding to mucin [25]. Binding between OligoG CF-5/20 and CF mucins was also previously characterized using FTIR, demonstrating an interaction between OligoG CF-5/20 and the carbonyl group within the peptide link

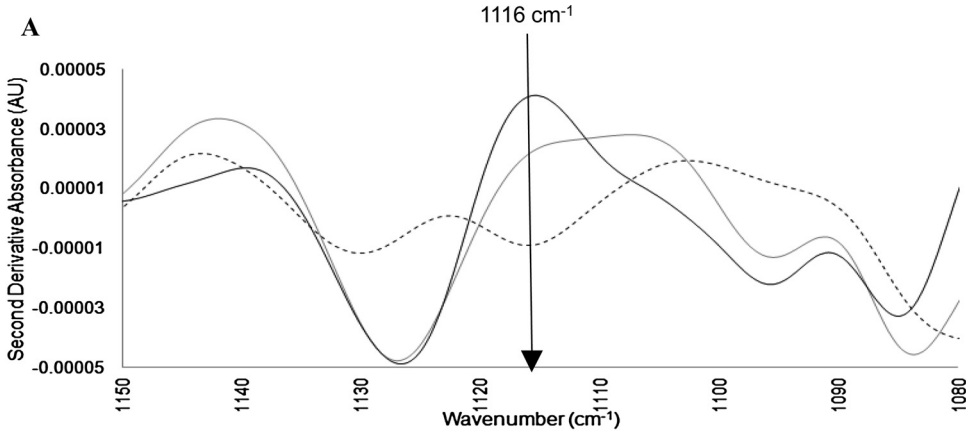

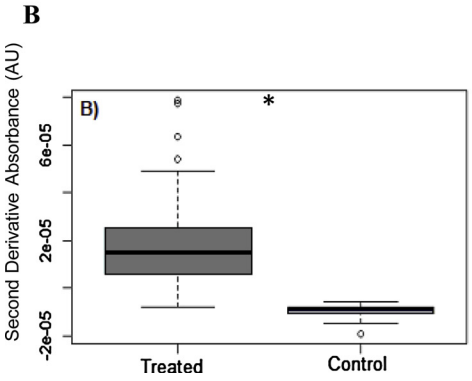

Fig. 3. Mean second derivative spectra for OligoG CF-5/20 treated and untreated sputum surrounding 1116 cm^{-1} indicating IR absorbance from sulphated-Lewis x antigen. (a) The IR peak at 1116 cm^{-1} was lost following OligoG CF-5/20 incubation. The new peak occurring at 1096 cm^{-1} in the treated spectrum is suggestive of interaction between OligoG CF-5/20 and sulphated- sulphated-Lewis x antigen. (b) Boxplots of second derivative negative peak height distributions centered around 1116 cm^{-1} in untreated and treated samples respectively. Treated sputum, solid grey line; untreated sputum, black dashed line; OligoG CF-5/20, light-grey dashed line. *P < 0.008, mean of n = 3 replicates.

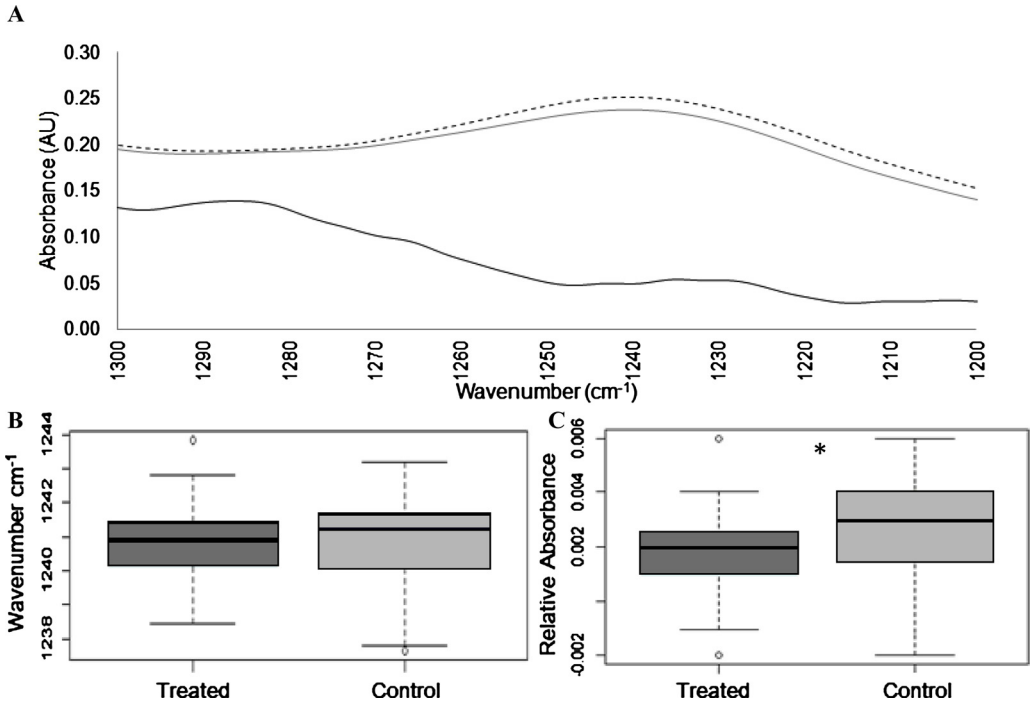

Fig. 4. Mean raw absorbance at 1240 cm^{-1}. (a) Mean treated and untreated spectra showing lower absorbance in the treated spectrum. Boxplots showing the distribution of (b) wavenumber and (c) relative absorbance in untreated and treated samples centered around 1240 cm^{-1}. Treated sputum, solid grey line; untreated sputum, black dashed line; OligoG CF-5/20, light-grey dashed line. *P < 0.008, mean of n = 3 replicates.

of the mucin protein backbone found in the Amide I region [25]. It is possible that the experimental conditions, namely the drying of the sputum to form a thin film, could influence the protein secondary structure and therefore the peak positions. However, there are a number of publications which show that comparable protein secondary structure information is derived from circular dichroism and FTIR based experiments on protein solutions and on thin films [44–47]. Therefore, it is reasonable to hypothesise that the experimentally required drying of the sputum was unlikely to cause alterations to the secondary structure of the mucins in our current study.

In the present study, we did not observe statistically significant ($P > 0.008$) shifts in peak position around 1652cm^{-1} (Fig. 5b i-iii), and we could not observe a statistically significant decrease in second derivative peak height at 1637 cm^{-1} ($P < 0.05$, but $P > 0.008$) in the OligoG CF-5/20 treated samples (Fig. 5c iii). It is probable that the small sample size used in the current study may contribute towards this

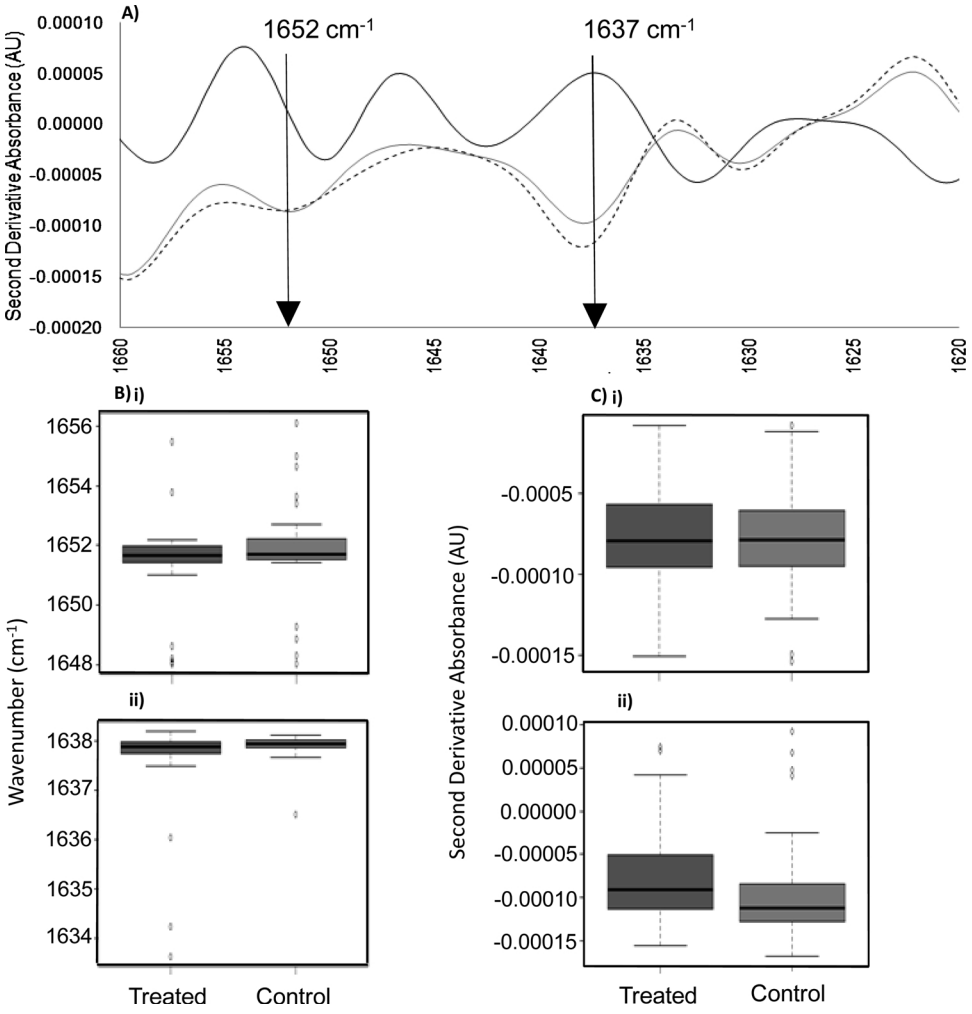

Fig. 5. Mean second derivative spectra for OligoG CF-5/20 treated and untreated sputum within the Amide 1 region between 1628 cm^{-1} and 1664 cm^{-1}. (a) A wavenumber shift at 1652 cm^{-1} related to random coil secondary structure and absorbance change at 1637 cm^{-1} related to β-sheet structure were observed. (b) Boxplots showing the distribution of peak positions in untreated and treated samples centered around i)1652 cm^{-1} and ii) 1637 cm^{-1}. (c) Boxplots showing the distribution of second derivative absorbance in untreated and treated samples centered around i)1652 cm^{-1} and ii) 1637 cm^{-1}. Treated sputum, solid grey line; untreated sputum, black dashed line; OligoG CF-5/20, light-grey dashed line.

lack of significance. Previous molecular modelling observations have shown that OligoG is able to alter the structure of mucus and modulate mucin assembly [25]. We hypothesized this to be as a result of hydrogen bonding between OligoG CF-5/20 and the peptide backbone causing a conformational change in the β-sheet secondary structure of the peptide backbone. The closeness to significance shown in the current study is promising and a larger study may demonstrate significance. We also hypothesize that steric hindrance may have contributed to the lack of significant change noted between OligoG CF-5/20 incubated sputum and control sputum spectra at the random coil associated wavenumber, 1652 cm^{-1}.

3.3. Clinical data analysis

The use of portable FTIR has recently been shown to predict acute episodes of chronic obstructive pulmonary disease (COPD) [18] and to the facilitate detection of lung cancer [31,48–50]. A potential role for FTIR in CF is not unreasonable given the changes seen in CF mucus with DNA, F-actin, mucin structure, and rheology, which have been associated with pulmonary exacerbations [51].

All patients (except one) who provided induced sputum samples were taking antibiotics (Table 1). No correlation was found between the wavenumber changes reported here and antibiotic use, sex, age, use of rhDNase I or forced expiratory volume in 1 s (FEV_1).

FTIR analysis, however, does have limitations: It cannot determine the exact molecular structure of compounds, and some vibrations detected by FTIR are attributable to multiple chemical groups. These limitations are being overcome by the development of an FTIR reference library for monosaccharides [18]. Moreover, the IR spectral pattern of untreated CF sputum within the fingerprint region in the current study were shown to be highly similar to that seen in sputum from COPD patients [18]. As sialylation and sulphation of the Lewis x antigen is associated with respiratory disease, FTIR could be further developed to monitor the treatment of CF patients, and identify potential mucosal changes prior to pulmonary exacerbations [18]. However, there is considerable heterogeneity in CF sputum samples, so experiments should be performed with sufficient replication to identify potential outliers [19]. Despite this inherent heterogeneity, FTIR analysis in the current study showed remarkable intra-sample reproducibility, and confirmed key specific binding sites for OligoG CF-5/20 with mucin glycan moieties and the peptide backbone.

4. Conclusion

These findings demonstrate the use of FTIR analysis to study the interaction of alginate OligoG CF-5/20 with glycan moieties and the peptide backbone of mucin molecules in CF sputum. As increases in sulphation within CF mucins are associated with infection and reduced pulmonary function, this finding suggests a potential mechanism whereby OligoG CF-5/20 modifies the viscoelastic properties of CF sputum.

It is known that patients with cystic fibrosis have sub-optimal adherence to long-term inhaled therapies, but this can be improved through the use of electronic monitoring [52]. The current study shows how a simple FTIR-based protocol can be utilized to detect interaction between OligoG CF-5/20 and sputum mucins. It is feasible that FTIR

analysis could be employed to monitor patient adherence to therapy through detection of OligoG CF-5/20 in expectorated sputum, and allow healthcare providers to give additional support to patients who show poor compliance with essential treatments.

Acknowledgments

The authors would like to express their sincere thanks to the patients who donated samples. We thank Dr Aaran Lewis and Mr Sam Lewis for their training and guidance on the FTIR. MFP, JO, PDR, KEH and DWT were funded from the European Union via the Eurostars (TM) Programme and the European Social Fund, Research Council of Norway, Cystic Fibrosis Foundation US and AlgiPharma AS. PL and CB were supported through research grants provided by Health Care Research Wales and the Welsh Government's Health Technology and Telehealth Fund. DWT and PDR has, with KEH, received research funding from AlgiPharma AS. PDR is the research director of AlgiPharma AS. The other authors have no conflicts of interest to disclose. Sputum samples were collected by JF, IK and IJMD with ethical approval (CF Sputum Induction Trial [CF-SpIT] UKCRN: 14615). We confirm that all authors have read the journal's authorship agreement and policy on disclosure of potential conflicts of interest.

References

[1] D. Taylor-Robinson, O. Archangelidi, S.B. Carr, R. Cosgriff, E. Gunn, R.H. Keogh, A. MacDougall, S. Newsome, D.K. Schluter, S. Stanojevic, D. Bilton, Data resource profile: the UK cystic fibrosis registry, Int. J. Epidemiol. (2017).
[2] CF Trust, UK Cystic Fibrosis Registry Annual Data Report 2016, (2016).
[3] G.R. Cutting, Cystic fibrosis genetics: from molecular understanding to clinical application, Nat. Rev. Genet. 16 (2015) 45–56.
[4] CF Foundation, Cystic Fibrosis Foundation Patient Registry Annual Data Report 2011, Cystic Fibrosis Foundation, 2012.
[5] A. Folkesson, L. Jelsbak, L. Yang, H.K. Johansen, O. Ciofu, N. Hoiby, S. Molin, Adaptation of *Pseudomonas aeruginosa* to the cystic fibrosis airway: an evolutionary perspective, Nat. Rev. Microbiol. 10 (2012) 841–851.
[6] S.K. Lai, Y.Y. Wang, D. Wirtz, J. Hanes, Micro- and macrorheology of mucus, Adv. Drug Deliv. Rev. 61 (2009) 86–100.
[7] M.C. Rose, J.A. Voynow, Respiratory tract mucin genes and mucin glycoproteins in health and disease, Physiol. Rev. 86 (2006) 245–278.
[8] M.O. Henke, G. John, M. Germann, H. Lindemann, B.K. Rubin, MUC5AC and MUC5B mucins increase in cystic fibrosis airway secretions during pulmonary exacerbation, Am. J. Respir. Crit. Care Med. 175 (2007) 816–821.
[9] J.E. Phillips, N.R. Case, C. Celly, R.W. Chapman, J.A. Hey, M. Minnicozzi, An enzyme-linked immunosorbent assay (ELISA) for the determination of mucin levels in bronchoalveolar lavage fluid, J. Pharmacol. Toxicol. Methods 53 (2006) 160–167.
[10] M. King, Mucus and its role in airway clearance and cytoprotection, Hamilton, Ontario, Canada: BC Decker (2005) 409–416.
[11] G. Lamblin, S. Degroote, J.M. Perini, P. Delmotte, A.E. Scharfman, M. Davril, J.M. Lo-Guidice, N. Houdret, V. Dumur, A. Klein, P. Roussel, Human airway mucin glycosylation: a combinatory of carbohydrate determinants which vary in cystic fibrosis, Glycoconjugate J. 18 (2001) 661–684.
[12] M. King, B.K. Rubin, Pharmacological approaches to discovery and development of new mucolytic agents, Adv. Drug Deliv. Rev. 54 (2002) 1475–1490.
[13] N. Jonckheere, I. Van Seuningen, The membrane-bound mucins: how large o-glycoproteins play key roles in epithelial cancers and hold promise as biological tools for gene-based and immunotherapies, Crit. Rev. Oncog. 14 (2008) 177–196.
[14] S.K. Linden, P. Sutton, N.G. Karlsson, V. Korolik, M.A. McGuckin, Mucins in the mucosal barrier to infection, Mucosal Immunol. 1 (2008) 183–197.
[15] M.F. Kagnoff, L. Eckmann, Epithelial cells as sensors for microbial infection, J. Clin. Invest. 100 (1997) 6–10.
[16] J.G. Widdicombe, Airway liquid: a barrier to drug diffusion? Eur. Resp. J. 10 (1997) 2194–2197.
[17] R. Bansil, B.S. Turner, Mucin structure, aggregation, physiological functions and biomedical applications, Curr. Opin. Colloid Interface Sci. 11 (2006) 164–170.
[18] A.T. Lewis, K. Jones, K.E. Lewis, S. Jones, P.D. Lewis, Detection of lewis antigen structural change by FTIR spectroscopy, Carbohydr. Polym. 92 (2013) 1294–1301.
[19] P.G. Bhat, D.R. Flanagan, M.D. Donovan, Drug diffusion through cystic fibrotic mucus: steady-state permeation, rheologic properties, and glycoprotein morphology, J. Pharm. Sci. 85 (1996) 624–630.
[20] S. Degroote, M.P. Ducourouble, P. Roussel, G. Lamblin, Sequential biosynthesis of sulfated and/or sialylated lewis x determinants by transferases of the human bronchial mucosa, Glycobiology 9 (1999) 1199–1211.
[21] B.Y. Xia, J.A. Royall, G. Damera, G.P. Sachdev, R.D. Cummings, Altered o-glycosylation and sulfation of airway mucins associated with cystic fibrosis, Glycobiology 15 (2005) 747–775.
[22] M. Davril, S. Degroote, P. Humbert, C. Galabert, V. Dumur, J.J. Lafitte, G. Lamblin, P. Roussel, The sialylation of bronchial mucins secreted by patients suffering from cystic fibrosis or from chronic bronchitis is related to the severity of airway infection, Glycobiology 9 (1999) 311–321.
[23] P. Delmotte, S. Degroote, J.J. Lafitte, G. Lamblin, J.M. Perini, P. Roussel, Tumor necrosis factor alpha increases the expression of glycosyltransferases and sulfotransferases responsible for the biosynthesis of sialylated and/or sulfated lewis x epitopes in the human bronchial mucosa, J. Biol. Chem. 277 (2002) 424–431.
[24] C.T. Nordgard, K.I. Draget, Oligosaccharides as modulators of rheology in complex mucous systems, Biomacromolecules 12 (2011) 3084–3090.
[25] M.F. Pritchard, L.C. Powell, G.E. Menzies, P.D. Lewis, K. Hawkins, C. Wright, I. Doull, T.R. Walsh, E. Onsoyen, A. Dessen, R. Myrvold, P.D. Rye, A.H. Myrset, H.N.E. Stevens, L.A. Hodges, G. MacGregor, J.B. Neilly, K.E. Hill, D.W. Thomas, A new class of safe oligosaccharide polymer therapy to modify the mucus barrier of chronic respiratory disease, J. Mol. Pharm. Org. Process Res. 13 (2016) 863–872.
[26] S. Khan, A. Tondervik, H. Sletta, G. Klinkenberg, C. Emanuel, E. Onsoyen, R. Myrvold, R.A. Howe, T.R. Walsh, K.E. Hill, D.W. Thomas, Overcoming drug resistance with alginate oligosaccharides able to potentiate the action of selected antibiotics, Antimicrob. Agents Chemother. 56 (2012) 5134–5141.
[27] M.F. Pritchard, L.C. Powell, A.A. Jack, K. Powell, K. Beck, H. Florance, J. Forton, P.D. Rye, A. Dessen, K.E. Hill, D.W. Thomas, A low molecular weight alginate oligosaccharide disrupts pseudomonal microcolony formation and enhances antibiotic effectiveness, Antimicrob. Agents Chemother. (61) (2017) e00762–17.
[28] L.C. Powell, M.F. Pritchard, C. Emanuel, E. Onsoyen, P.D. Rye, C.J. Wright, K.E. Hill, D.W. Thomas, A nanoscale characterization of the interaction of a novel alginate oligomer with the cell surface and motility of Pseudomonas aeruginosa, Am. J. Respir. Cell Mol. Biol. 50 (2014) 483–492.
[29] M. Sletmoen, G. Maurstad, C.T. Nordgard, K.I. Draget, B.T. Stokke, Oligoguluronate induced competitive displacement of mucin-alginate interactions: relevance for mucolytic function, Soft Matter 8 (2012) 8413–8421.
[30] S.P. Lewis, A.T. Lewis, P.D. Lewis, Prediction of glycoprotein secondary structure using atr-ftir, Vib. Spectrosc. 69 (2013) 21–29.
[31] P.D. Lewis, K.E. Lewis, R. Ghosal, S. Bayliss, A.J. Lloyd, J. Wills, R. Godfrey, P. Kloer, L.A.J. Mur, Evaluation of FTIR spectroscopy as a diagnostic tool for lung cancer using sputum, BMC Cancer 10 (2010) 640.
[32] A. Scharfman, P. Delmotte, J. Beau, G. Lamblin, P. Roussel, J. Mazurier, Sialyl-le(x) and sulfo-sialyl-le(x) determinants are receptors for P. Aeruginosa, Glycoconj. J. 17 (2000) 735–740.
[33] J. Mendicino, S. Sangadala, Synthesis of sulfated oligosaccharides by cystic fibrosis trachea epithelial cells, Mol. Cell. Biochem. 201 (1999) 141–149.
[34] R. Ramphal, S.K. Arora, Recognition of mucin components by Pseudomonas aeruginosa, Glycoconj. J. 18 (2001) 709–713.
[35] Y.L. Zhang, B. Doranz, J.R. Yankaskas, J.F. Engelhardt, Genotypic analysis of respiratory mucous sulfation defects in cystic fibrosis, J. Clin. Invest. 96 (1995) 2997–3004.
[36] C.V. Robinson, M.R. Elkins, K.M. Bialkowski, D.J. Thornton, M.A. Kertesz, Desulfurization of mucin by *Pseudomonas aeruginosa*: influence of sulfate in the lungs of cystic fibrosis patients, J. Med. Microbiol. 61 (2012) 1644–1653.
[37] B.L. Schulz, A.J. Sloane, L.J. Robinson, S.S. Prasad, R.A. Lindner, M. Robinson, P.T. Bye, D.W. Nielson, J.L. Harry, N.H. Packer, N.G. Karlsson, Glycosylation of sputum mucins is altered in cystic brosis patients, Glycobiology 17 (2007) 698–712.
[38] R.A. Cone, Barrier properties of mucus, Adv. Drug Deliv. Rev. 61 (2009) 75–85.
[39] S.K. Lai, Y.-Y. Wang, J. Hanes, Mucus-penetrating nanoparticles for drug and gene delivery to mucosal tissues, Adv. Drug Deliv. Rev. 61 (2009) 158–171.
[40] C.T. Nordgard, U. Nonstad, M.O. Olderoy, T. Espevik, K.I. Draget, Alterations in mucus barrier function and matrix structure induced by guluronate oligomers, Biomacromolecules 15 (2014) 2294–2300.
[41] R.K. Willits, W.M. Saltzman, Synthetic polymers alter the structure of cervical mucus, Biomaterials 22 (2001) 445–452.
[42] A.T.Y. Yeung, A. Parayno, R.E.W. Hancock, Mucin promotes rapid surface motility in Pseudomonas aeruginosa, Mbio 3 (2012) e00073–00012.
[43] A.A. Jack, S. Khan, L.C. Powell, M.F. Pritchard, K. Beck, H. Sadh, L. Sutton, A. Cavaliere, H. Florance, P.D. Rye, D.W. Thomas, K.E. Hill, Alginate oligosaccharide-induced modification of the *lasI-lasR* and *rhlI-rhlR* quorum-sensing systems in *Pseudomonas aeruginosa*, Antimicrob. Agents Chemother. 62 (2018) e02318–02317.
[44] E. Goormaghtigh, R. Gasper, A. Bénard, A. Goldsztein, V. Raussens, Protein secondary structure content in solution, films and tissues: redundancy and complementarity of the information content in circular dichroism, transmission and ATR FTIR spectra, Biochimica et Biophysica Acta - Proteins and Proteomics 1794 (9) (2009) 1332–1343, https://doi.org/10.1016/j.bbapap.2009.06.007.
[45] S.P. Lewis, A.T. Lewis, P.D. Lewis, Prediction of glycoprotein secondary structure using ATR-FTIR, Vib. Spectrosc. 69 (2013) 21–29, https://doi.org/10.1016/j.vibspec.2013.09.001.
[46] R. Pribić, I.H.M. van Stokkunm, D. Chapman, P.I. Haris, M. Bloemendal, Protein secondary structure from fourier transform infrared and/or circular dichroism spectra, Anal. Biochem. 214 (1993) 366–378.
[47] W.K. Surewicz, H.H. Mantsch, D. Chapman, Determination of protein secondary structure by fourier transform infrared spectroscopy: a critical assessment, Biochemistry 32 (2) (1993) 389–394.
[48] K. Yano, S. Ohoshima, Y. Gotou, K. Kumaido, T. Moriguchi, H. Katayama, Direct measurement of human lung cancerous and noncancerous tissues by Fourier Transform infrared microscopy: can an infrared microscope be used as a clinical tool? Anal, Biochem. 287 (2000) 218–225.
[49] K. Yano, S. Ohoshima, Y. Shimizu, T. Moriguchi, H. Katayama, Evaluation of glycogen level in human lung carcinoma tissues by an infrared spectroscopic method, Cancer Lett. 110 (1996) 29–34.
[50] H.P. Wang, H.C. Wang, Y.J. Huang, Microscopic ftir studies of lung cancer cells in pleural fluid, Sci. Total Environ. 204 (1997) 283–287.
[51] J.T. Ma, C. Tang, L. Kang, J.A. Voynow, B.K. Rubin, Cystic fibrosis sputum rheology correlates with both acute and longitudinal changes in lung function, Chest (2018).
[52] S. Narayanan, J.G. Mainz, S. Gala, H. Tabori, D. Grossoehme, Adherence to therapies in cystic fibrosis: a targeted literature review, Expert Rev. Respir. Med. 11 (2) (2017) 129–145.